

Inhibition of miRNA-27b enhances neurogenesis via AMPK activation in a mouse ischemic stroke model

Zhengang Wang¹ , Yimei Yuan¹, Zhaoguang Zhang² and Kuiying Ding³

¹ Department of Neurosurgery, Affiliated Hospital of Weifang Medical University, China

² Department of Ultrasonography, Affiliated Hospital of Weifang Medical University, China

³ Technology Center, Weifang Entry-exit Inspection and Quarantine Bureau, China

Keywords

AMPK; hippocampal dentate gyrus; miRNA-27b; neurogenesis; stroke; subventricular zone

Correspondence

Z. Wang, Department of Neurosurgery, Affiliated Hospital of Weifang Medical University, 2428 Yuhe Rd, Weifang, Shandong 261000, China
Tel: +86 0536 3081299
E-mail: zhengang.wang62@yahoo.com

(Received 15 October 2018, revised 21 January 2019, accepted 25 January 2019)

doi:10.1002/2211-5463.12614

Stroke is a leading cause of death and disability, but treatment options remain limited. Recent studies have suggested that cerebral ischemia-induced neurogenesis plays a vital role in post-stroke repair. Overactivation of AMP-activated protein kinase (AMPK), a master sensor of energy balance, has been reported to exacerbate neuron apoptosis, but the role of chronic AMPK stimulus in post-stroke recovery remains unclear. MicroRNAs have emerged as regulators of neurogenesis and have been reported to be involved in neurological function. In this study, we verified that miR-27b directly targets AMPK and inhibits AMPK expression. In cultured neural stem cells, miR-27b inhibitor improved proliferation and differentiation via the AMPK signaling pathway, but did not have an obvious effect on cell viability under oxygen and glucose deprivation conditions. In a mouse middle cerebral artery occlusion model, administration of miR-27b inhibitor significantly enhanced behavioral function recovery and spatial memory. Up-regulation of neurogenesis was observed both in the subventricular zone and in the hippocampal dentate gyrus. Collectively, our data suggest that miR-27b inhibition promotes recovery after ischemic stroke by regulating AMPK activity. These findings may facilitate the development of novel therapeutic strategies for stroke.

Stroke is one of leading causes of death and long-term disability worldwide [1]. Ischemic stroke accounts for more than 80% of stroke, local ischemia and a hypoxic environment induce neuronal cell apoptosis, necrosis and other metabolism-related disorders. At present, recombinant tissue plasminogen activator is the only FDA-approved treatment for acute ischemic stroke, but a narrow therapeutic window limits its clinic usage [2]. Meanwhile, there is no neuroprotective agent that has shown prospective results in clinical trials.

Brain repair processes after ischemic stroke are attracting more attention. Accumulating studies have suggested that cerebral ischemia-induced neurogenesis [3–5], which occurs mainly in the subventricular zone (SVZ) and subgranular zone in hippocampal dentate gyrus (DG) [6], might give rise to a cure strategy for recovery of brain function [7,8]. In DG, newborn neurons are continuously produced throughout adulthood [9–11]. A manipulated increase of neurogenesis in DG was reported to improve synaptic plasticity and memory

Abbreviations

ACC, acetyl-CoA carboxylase; AICAR, 5-aminoimidazole-4-carboxamide ribonucleotide; AMPK, AMP-activated protein kinase; BrdU, 5-bromo-2'-deoxyuridine; CBF, cerebral blood flow; DCX, doublecortin; DG, dentate gyrus; DMEM, Dulbecco's modified Eagle's medium; EBSS, Earle's Balanced Salt Solution; MCAo, middle cerebral artery occlusion; miR, microRNA; miRNA, microRNA; mTOR, mechanistic target of rapamycin; MTT, 3-(4,5-dimethylthiazol-2-yl)-2,5-diphenyl-tetrazolium bromide; NeuN, neuronal nuclei; NSC, neural stem cell; OGD, oxygen–glucose deprivation; PKC ζ/λ , protein kinase C ζ/λ ; SVZ, subventricular zone; TTC, 2,3,5-triphenyltetrazolium chloride; Tuj1, class III β -tubulin; UTR, untranslated region; WT, wild-type.

[12,13]. For now, it remains a challenge to amplify this process to enhance neurological function after injury.

The role that AMP-activated protein kinase (AMPK) plays in ischemic brain remains a matter of debate. Several studies reported that AMPK activation is detrimental, since it enhances energy-consuming pathways that further contribute to the death of injured neuronal cells [14–16]. Meanwhile, Kuramoto *et al.* [17] suggested that AMPK leads to neuroprotection through functional modulation of the GABA_B receptor. Besides the effects on neural apoptosis and mortality, AMPK has been reported to play a dual role in generation of new neurons; the divergent effects result from the duration and extent of AMPK activation [18,19]. The use of low dose 5-aminoimidazole-4-carboxamide ribonucleotide (AICAR; an AMPK direct activator) enhanced neurogenesis and cognition, while high dose AICAR impaired cognition and induce cell apoptosis [20].

MicroRNAs (miRNAs) are small non-coding RNAs of ~ 20 nucleotides that act as post-transcriptional regulators of their targets mRNAs [21]. The studies of other groups have indicated that miRNAs play an important role in neuroprotection and post-stroke recovery [22–27]. It has been demonstrated that miR-27b was markedly reduced in numerous types of cancer and exerted anti-tumor effects by suppressing cell proliferation [28], but its effects on neurogenesis after ischemic stroke have not been investigated.

In the present study, we confirmed the direct targeting of miR-27b on AMPK α 2, the main effective AMPK α isoform in ischemic brain [14]. We down-regulated miR-27b expression in cultured neural stem cells (NSCs) and observed mild stimulation of AMPK. In conditions of ischemia and hypoxia, the enhancement of AMPK activity by anti-miR-27b improved neurogenesis and post-stroke neurological function recovery.

Materials and methods

Luciferase assay

Luciferase reporter plasmid carrying wild-type (WT) or mutant AMPK α 2 gene (*PRKAA2*-3'UTR WT/Mu) was constructed and cloned in a pEZX-MT06 vector (Genecopoeia, Rockville, MD, USA). Point mutations were made in the miR-27b binding site of 3'-untranslated region (UTR) of the AMPK α 2 gene (Fig. 1A). HEK293T cells (ATCC, Manassas, VA, USA) were seeded in 24-well plate (10^5 /well) and co-transfected with 100 ng miR-27b mimics (UUCACA GUGGCUAAGUUCUGC; Dharmacon, Lafayette, CO, USA) or 100 ng miRNA mimic negative control (Dharmacon, cat. no.: CN-001000-01-05, USA) and WT or mutant AMPK α 2 (100 ng) using Lipofectamine-2000 transfection

reagent according to the manufacturer's instructions (Life Technologies, Carlsbad, CA, USA). About 48 h later, cells were lysed and luciferase activity was detected using a dual-luciferase assay kit (Genecopoeia) and luminometer (Thermo Fisher Scientific, Waltham, MA, USA).

Neural stem cells culture

Isolation of mouse NSCs was performed as described previously [29,30]. Mouse brains were cut sagittally and SVZ was dissociated from lateral ventricles. Tissue was gently minced and digested in 0.05% trypsin (Sigma-Aldrich, St. Louis, MO, USA) in Dulbecco's modified Eagle's medium (DMEM; 1 mL per 100 mg tissue) at 37 °C for 1 h. Digestion was stopped with an equal volume of 0.1% trypsin inhibitor (Sigma-Aldrich). The solution was centrifuged at 300 g for 10 min, the supernatant discarded, and the pellet suspended in proliferation medium: DMEM/F12 (Life Technologies) supplemented with epidermal growth factor (20 ng·mL⁻¹; R&D Systems, Minneapolis, MN, USA), fibroblast growth factor (10 ng·mL⁻¹; R&D System), N2 supplement (1%; Thermo Fisher Scientific), B27 supplement (3%; Thermo Fisher Scientific) and glutamax (1% Thermo Fisher Scientific). The medium was half changed twice a week. When spherical structures formed, the spheres were mechanically dissociated to a single cell suspension and seeded to 1% laminin-coated plates. The next day, NSCs were transfected with 10 μ M miR-27b inhibitor or 10 μ M miR inhibitor negative control (anti-miR-27b inhibitor, 5'-GCAGAACUUAGC-CACUGUGAA-3'; anti-miR-NC, 5'-CAGUACUUUUGU-GUAGUACAA-3', synthesized by RiboBio Co., Guangzhou, China) using Lipofectamine-2000 [31]. About 48 h later, NSCs could be used for cell viability assay, differentiation induction and immunostaining.

Cortical neuronal culture

Cortical neurons were isolated from 18-day-old male C57BL/6 mice as described [32]. Neurons were dissociated with 0.125% trypsin and pre-purified by density gradient. Neurons were seeded at a density of ~ 2500 cells·mm⁻² and cultured using DMEM containing 20% FBS. On the next day, the medium was changed to neuron-basal medium supplemented with 2% B27 (R&D Systems). Neurons were cultured for another 3 days and used for cell viability assay.

Oxygen–glucose deprivation and cell viability assay

Cortical neurons and NSCs were washed with PBS three times, then placed in glucose-free Earle's Balanced Salt Solution (EBSS) buffer and stored in an anoxic chamber filled with 95% N₂ and 5% CO₂ for 6 h [33]. For the control, cells remained in normoxic conditions. The cell survival rates were determined using the 3-(4,5-dimethylthiazol-2-yl)-2,5-diphenyl-

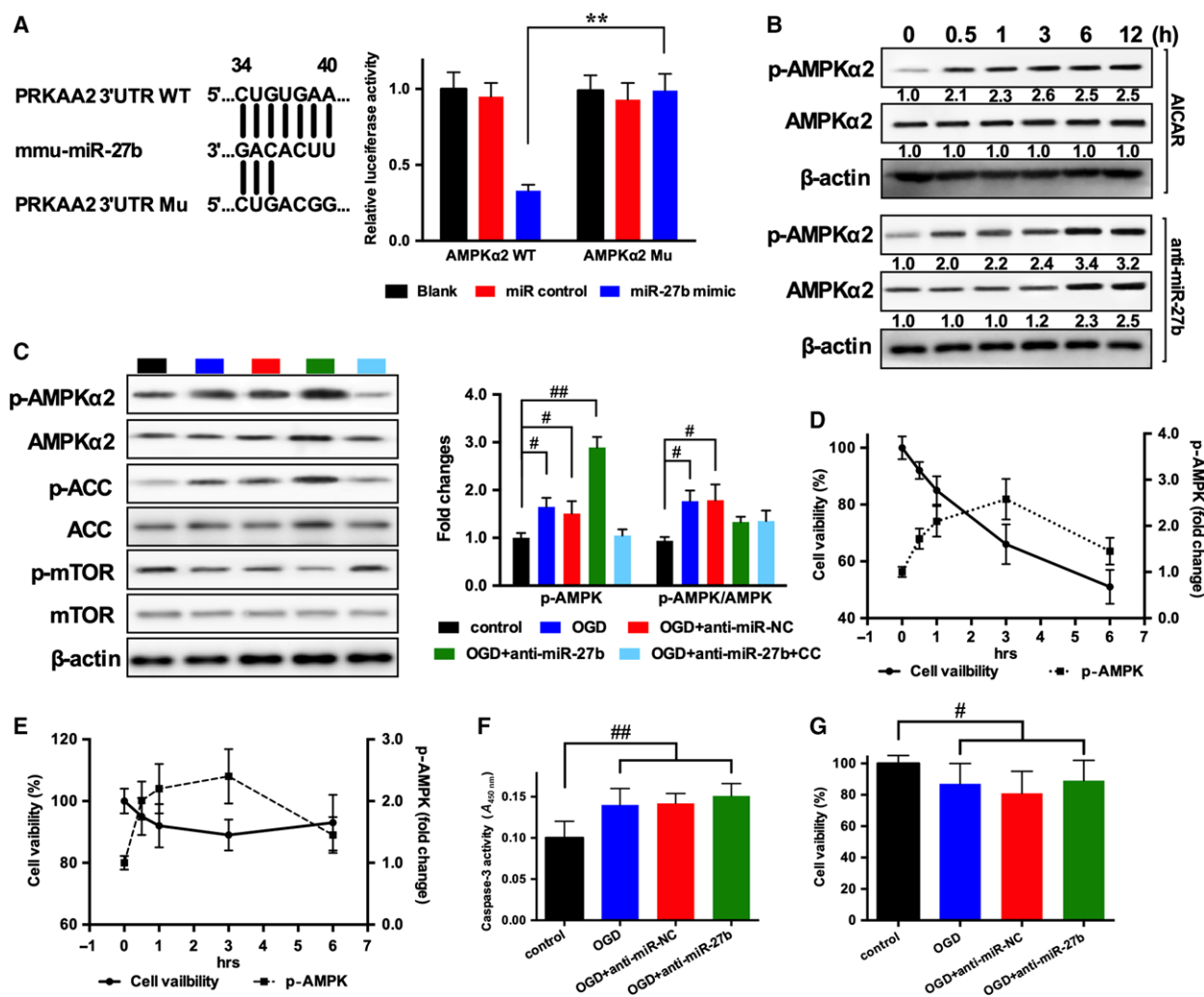


Fig. 1. Effects of AMPK activation on neuron and NSC viability in OGD treatment. (A) Schematic diagram of miR-27b binding site in WT AMPK α 2 (*PRKAA2*) 3'UTR fragment and design of mutated sequence; and luciferase reporter assay of WT or mutant 3'UTR of *PRKAA2* with miR control or miR-27b mimic in HEK 293T cells. (B) Time course of AMPK α 2 and p-AMPK α 2 expression in NSCs treated with AICAR or transfected with anti-miR-27b. (C) Western blot analysis of AMPK α 2, p-AMPK α 2, ACC, p-ACC, mTOR and p-mTOR expression and their quantitative data in NSCs transfected with miR negative control, anti-miR-27b, or anti-miR-27b with added compound C (1 μ M) at 6 h. (D, E) Time courses of OGD-induced AMPK activation and cell viability in cortical neurons (D) and NSCs (E). (F) Caspase-3 activity tested using a Caspase-3 Colorimetric Assay kit. (G) MTT assay was used to test the viability of NSCs treated with anti-miR-27b in OGD condition. $n = 3$ /group. The data are expressed as mean \pm SEM, $**P < 0.01$ WT vs Mu; $\#P < 0.05$, $##P < 0.01$ vs control (one-way ANOVA followed by *post hoc* Tukey's test).

tetrazolium bromide (MTT) assay. MTT was added into the medium at a final concentration of 0.5 mg·mL⁻¹ and incubated at 37 °C for 4 h. The MTT formazan was dissolved in DMSO and the absorbance was measured at 490 nm. Caspase-3 activity was tested using a Caspase-3 Colorimetric Assay kit (Abcam, Cambridge, MA, USA).

Immunofluorescence staining and quantification

Neural stem cells were transfected with anti-miR-27b or anti-miR-NC and cultured for another 5 days. To label the

dividing cells, 5 μ M 5-bromo-2'-deoxyuridine (BrdU; Sigma-Aldrich) was added to the proliferation medium and the cells were cultured for another 8 h. The cells were then fixed and incubated with rabbit anti-BrdU (1 : 2000; Abcam) overnight at 4 °C and then incubated with goat anti-rabbit IgG (FITC, 1 : 300; Abcam) for 2 h. The slides were washed and mounted using mounting medium (Vector Laboratories, Burlingame, CA, USA) containing 4',6-diamidino-2-phenylindole for nucleus staining. To detect production of neurons, NSCs were transfected as described above and cultured in differentiation medium (the proliferation

medium supplemented with 5% FBS, without any growth factors) for 5 days, then cells were fixed and blocked and incubated with mouse anti-neuron-specific class III β -tubulin (Tuj1, 1 : 300; Abcam) overnight at 4 °C. The next day, cells were washed and incubated with goat anti-mouse IgG (FITC, 1 : 300; Abcam) secondary antibody for 2 h. The slides were washed and mounted as above.

For quantification, BrdU⁺ or Tuj1⁺ and total cell numbers were counted in 10 random view fields/well and three wells/group under a $\times 20$ objective lens. The results were presented as the percentage of immunoreactive cells.

To determine neurogenesis *in vivo*, coronal sections of brains were stained with the following markers: rabbit anti-doublecortin (DCX; 1 : 100; Abcam), rabbit anti-neuronal nuclei (NeuN; 1 : 100; Abcam). Images were taken under a $\times 40$ objective lens, and five random view fields were chosen for each section. One-in-ten series of sections were stained for each animal.

Animal experimental procedures

All experimental procedures were carried out in accordance with the *Care and Use of Laboratory Animals Guide* from the Ministry of Public Health of China and approved by the medical ethics committee of Weifang Medical University and Shandong University. Male C57BL/6J mice (~10 weeks, 18–22 g, specific pathogen free) were purchased from Animal Centre of Shandong University. The animals were acclimatized for a week before surgery. On day 0, all mice underwent functional tests and performed permanent middle cerebral artery occlusion (MCAo; sham group only exposed arteries, no sutures were inserted) [31,34,35]. Briefly, animals were anesthetized and the common carotid artery, external carotid artery and internal carotid artery were exposed on the right side. An 8-0 nylon filament was inserted from the external carotid artery into the lumen of the internal carotid artery. Two hours later, the motor tests were re-done in a modified neurological severity score (mNSS) test (Table 1). The animals were randomly divided and received scores of 3–5 in the following three groups: MCAo, antagomir negative control (200 $\mu\text{g}\cdot\text{kg}^{-1}$, antagomir-NC; GenePharma, Shanghai, China) and antagomir-27b (200 $\mu\text{g}\cdot\text{kg}^{-1}$; GenePharma); $n = 15$ for each group. Antagomir negative control or antagomir-27b was i.v. injected and the same dose of antagomir was injected on days 7, 14 and 28. Cell proliferation was assessed using BrdU incorporation; five mice from each group were i.p. injected with 100 $\text{mg}\cdot\text{kg}^{-1}$ BrdU from day 21 to day 28 after MCAo. At the end of the study, these animals were perfused with saline and 4% paraformaldehyde, and then brains were removed for immunostaining. Five mice from each group were sacrificed and their brains removed for 2,3,5-triphenyltetrazolium chloride (TTC) staining. The other five animals were tested for cerebral blood flow (CBF) using laser Doppler flowmetry (LSFG-ANW, Softcare, Ltd., Fukuoka, Japan). Using the same filter and

image solution setting, relative blood flow in regions of interest from both the contralateral and the ipsilateral half brain was recorded and analyzed, and then mice were sacrificed and the brains removed for protein extraction and western blot analysis.

Behavioral tests

A modified neurological severity score test was performed before MCAo, and on days 1, 4, 7, 14 and 28 after MCAo according to a previous report [31, 36]. All animals were tested for motor and sensory abilities, balance, reflex and abnormal movements. The evaluation standard is shown in Table 1; higher scores represent severer injury and the maximum score is 14.

The Morris water maze was used as described [31,37]. A white swimming pool 150 cm in diameter was filled with water to a depth of 30 cm. Pool temperature was maintained at 25 ± 0.5 °C. The escape platform was placed in the center of one quadrant of the pool, 1 cm below the surface of the water. Mice were allowed to find the submerged platform within 90 s. If they failed, the mice were placed on the platform for another 15 s. On each training day, each mouse was released from four different start points. The training was repeated for five consecutive days. The escape latency and the time spent in the quadrant with the platform were recorded.

Table 1. Modified neurological severity score.

Tests	Points
Motor tests	
Raising rat by the tail	
Flexion of forelimb	1
Flexion of hindlimb	1
Head moved > 10° to vertical axis within 30 s	1
Placing rat on the floor	
Normal walking	0
Inability to walk straight	1
Circling toward the paretic side	2
Falling down on the paretic side	3
Sensory tests	
Placing test (visual and tactile test)	1
Proprioceptive test (deep sensation, pushing the paw against the table edge to stimulate limb muscles)	1
Beam balance tests	
Balances with steady posture	0
Grasps side of beam	1
Hugs the beam and one limb falls down from the beam	2
Hugs the beam and two limbs fall down from the beam, or spins on beam (> 60 s)	3
Attempts to balance on the beam but falls off (> 40 s)	4
Attempts to balance on the beam but falls off (> 20 s)	5
Falls off: no attempt to balance or hang on to the beam (< 20 s)	6

Western blot analysis

Samples were ground and lysed in RIPA buffer containing 1% protease inhibitor and 1% phosphatase inhibitor (Cell Signaling Technology, Beverly, MA, USA) and centrifuged for 12 min at 12 000 *g*, 4 °C to remove debris. A BCA assay was used to determine protein concentrations (Beyotime, Shanghai, China). About 50 µg total protein for each sample was separated by SDS/PAGE and transferred to PVDF membrane. Membranes were incubated with the following primary antibodies: AMPK α 2 (1 : 1000; Cell Signaling Technology), phospho (p)-AMPK α 2 (Thr172, 1 : 1000; Cell Signaling Technology), acetyl-CoA carboxylase (ACC) (1 : 1000; Cell Signaling Technology), p-ACC (Ser79, 1 : 1000; Cell Signaling Technology), mechanistic target of rapamycin (mTOR) (1 : 1000; Cell Signaling Technology), p-mTOR (Ser248, 1 : 1000; Cell Signaling Technology), protein kinase C ζ/λ (PKC ζ/λ) (1 : 1000; Cell Signaling Technology), p-PKC ζ/λ (Thr410/403, 1 : 1000; Cell Signaling Technology), and β -actin (1 : 1000; Abcam). Signals were visualized by enhanced ECL substrate (Beyotime).

Statistical analysis

All data are presented as the mean \pm standard error (SE). Data analysis was performed using PRISM 6 (GraphPad Software, San Diego, CA, USA). ANCOVA was used to analyze functional test data; non-parametric one-way ANOVA followed by a *post hoc* Tukey's test was used to compare the difference in cell viability data, immunofluorescence staining data, and western blot data among groups. Statistical significance was set at $P < 0.05$.

Results

MiR-27b directly targets AMPK α 2

MiR-27b was predicted to match the 3'UTR of *PRKAA2* (the gene encoding AMPK α 2) mRNA according to the gene sequence database at targets.org (Fig. 1A). We employed a luciferase assay to confirm the targeting relation of miR27b and AMPK α 2. In cells co-transfected with WT AMPK α 2 3'UTR (AMPK α 2 WT) and miR-27b mimic, luciferase activity was significantly decreased compared to miR control or mutant AMPK α 2 3'UTR (AMPK α 2 Mu), which indicated that AMPK α 2 is directly targeted by miR-27b (Fig. 1A).

The effect of AMPK activation by anti-miR-27b on NSCs

To test the effect of anti-miR-27b AMPK activation, AICAR (1 mM), Compound C (an AMPK inhibitor,

1 µM), and anti-miR-27b were administrated at the indicated dose and the NSC culture was exposed to oxygen–glucose deprivation (OGD). We compared the expression of p-AMPK α 2 in AICAR-treated and anti-miR-27b-transfected NSCs. AICAR enhanced p-AMPK α 2 expression starting at 0.5 h (2.1-fold) but AMPK α 2 expression was not affected. The effect of anti-miR-27b was detected at 6 h, and both p-AMPK α 2 and AMPK α 2 were significantly increased (3.4-fold and 2.3-fold, respectively; Fig. 1B). At 6 h, anti-miR-27b increased the expression of p-AMPK α 2 and p-ACC (a down-stream target of AMPK in which p-ACC level generally reflects the AMPK activity) (Fig. 1C). The AMPK–mTOR axis appears to have a role in neurodegenerative processes. The expression pattern of p-mTOR was the converse of that of p-AMPK, while total mTOR expression was not affected (Fig. 1C).

The effect of AMPK activation on cell viability in OGD treatment

AMP-activated protein kinase is known to be activated by energy deficiency. To determine the effect of activated AMPK on apoptosis, we examined the time course of AMPK activity and cell viability in OGD treatment. Both in cortical neurons and in NSCs, p-AMPK α 2 expression was significantly increased 0.5 h after OGD treatment and further enhanced at 6 h (Fig. 1D,E). OGD decreased neuron viability to 51% at 6 h (Fig. 1D). In NSCs, the time course for p-AMPK α 2 expression was similar to that in neurons, but cell viability was slightly decreased to 89% with OGD treatment (Fig. 1E). These data indicate that in a hypoxic environment, AMPK stimuli might play different roles in different cell types. Next, we prolonged the OGD to 24 h, and tested the NSC viability. In OGD-treated groups, cell numbers were slightly increased compared to control group; anti-miR-NC and anti-miR-27b treatments exerted no obvious effects on apoptosis (Fig. 1F,G).

AMPK activation by anti-miR-27b improved proliferation and differentiation of NSCs

NSCs cultured in growth medium were transfected with anti-miR-NC or anti-miR-27b, and another group of cells were transfected with miR-27b inhibitor with Compound C added (1 µM). Immunofluorescence staining showed that OGD increased the percentage of BrdU-positive cells compared with control group ($28.1 \pm 3.0\%$ vs $17.2 \pm 2.1\%$, $P < 0.05$) (Fig. 2A,B). Anti-miR-27b further up-regulated the BrdU⁺ cell

numbers by $55.4 \pm 6.3\%$. But the effect of anti-miR-27b was blocked by Compound C (%BrdU⁺ cells was $15.3 \pm 2.2\%$). Next, we tested differentiation of NSCs in all groups treated the same way as above. Except the control group, NSCs were cultured in an OGD incubator for 24 h followed by 4 days in normal conditions. The percentage of Tuj1-positive cells was increased after OGD treatment ($3.8 \pm 0.4\%$ vs $5.9 \pm 0.5\%$, $P < 0.05$). Anti-miR-27b further enhanced the production of new neurons to $13.5 \pm 2.1\%$. Compound C reduced the percentage Tuj1⁺ cells to $4.6 \pm 0.8\%$ (Fig. 2C,D). These data indicated that, AMPK activation by anti-miR-27b transfection induced NSCs proliferation and differentiated into new neurons.

Antagomir-27b improved neurological recovery in MCAo mice

To verify the effects of miR-27b inhibition in neurological outcomes after ischemic stroke. We treated mice with antagomir-27b to silence endogenous miR-27b after MCAo surgery, and observed neurological functional recovery. As shown in Fig. 3, the antagomir-27b group showed a better neurological functional recovery outcome compared to the MCAo group from day 4 and this lasted through the entire study period ($P < 0.05$, Fig. 3A). From day 28, we employed the Morris water maze test to assess the spatial memory of all groups. The escape latency time for finding a hidden platform in the group that went through MCAo

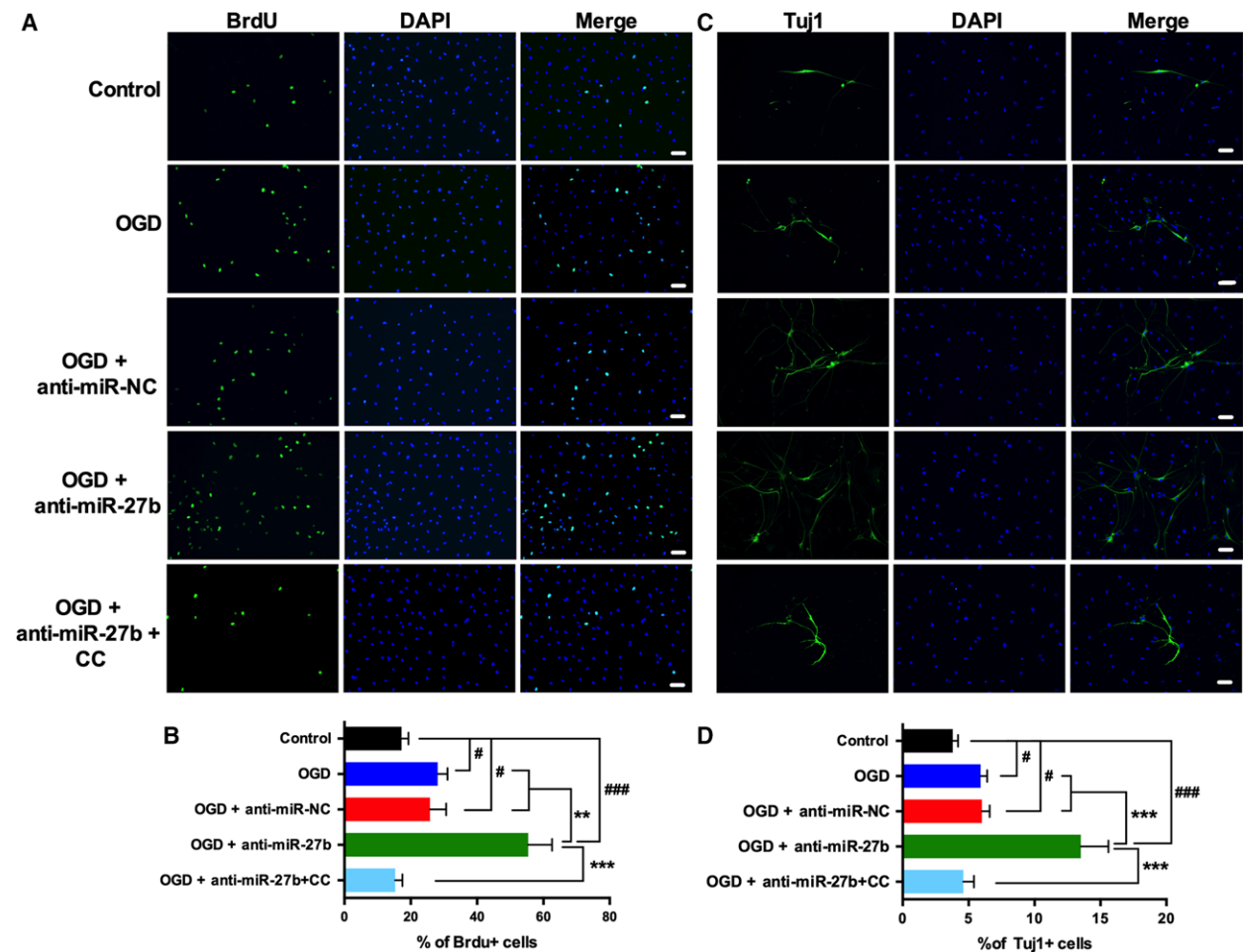


Fig. 2. MiR-27b is involved in neurogenesis via regulating AMPK activity. (A, B) Representative images and quantitative data of BrdU-positive cells in NSCs treated with miR-27b inhibitor negative control (anti-miR-NC), miR-27b inhibitor, or miR-27b inhibitor with Compound C (1 μ m). (C, D) Representative images and quantitative data of Tuj1-positive cells in NSCs treated the same way as above. $n = 3$ /group. The data are expressed as mean \pm SEM, # $P < 0.05$, ### $P < 0.001$ vs control; ** $P < 0.01$, *** $P < 0.001$ vs OGD + anti-miR-27b (one-way ANOVA followed by *post hoc* Tukey's test). Scale bar = 50 μ m.

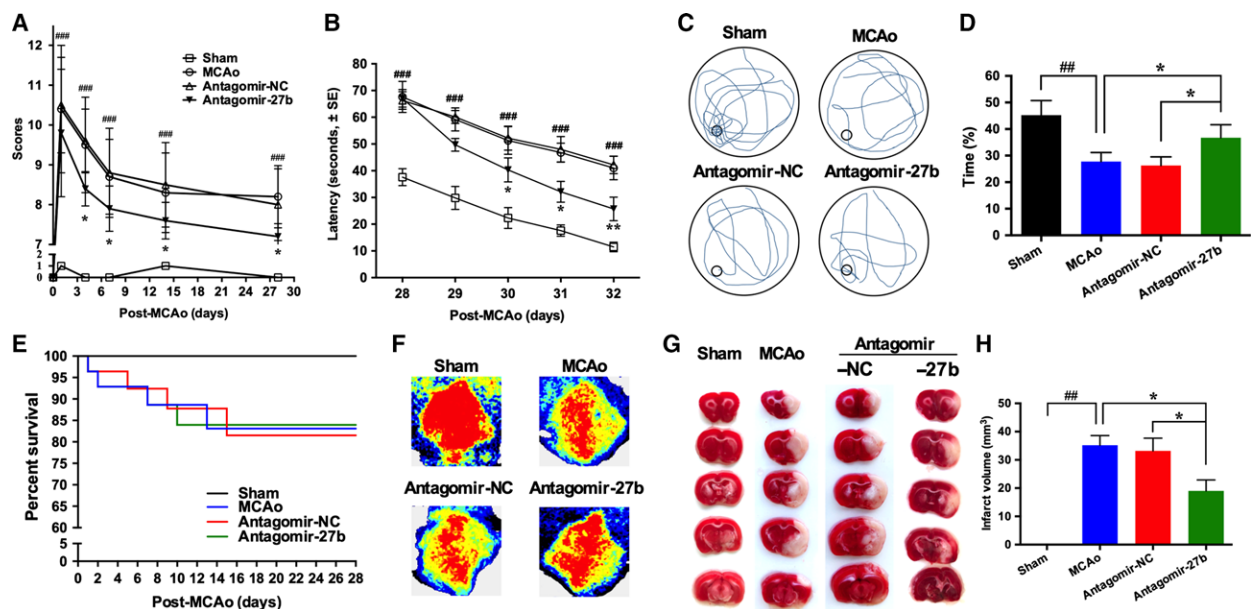


Fig. 3. Activation of AMPK by antagomir-27b improved neurological function after MCAo. (A) mNSS score test was performed at day 0, 1, 4, 7, 14 and 28 after MCAo. (B–D) Morris water maze test was performed from day 28 to day 32 after MCAo; average escape latency to the hidden platform is shown in (B), swim path is shown in (C), relative time of swimming in target quadrant (%) is shown in (D). (E) Survival from all groups after MCAo. (F) Representative images of CBF. (G, H) Representative images and quantification of mouse brain infarction volume from all groups after MCAo. $n = 10/\text{group}$ for functional tests, $n = 5/\text{group}$ for CBF test and TTC staining. The data are expressed as mean \pm SEM. $###P < 0.01$, $####P < 0.001$ vs sham; $*P < 0.05$, $**P < 0.01$ vs MCAo (ANCOVA).

surgery took much longer than in the sham group. Although the escape latency time of all groups showed decreased tendency during the training period of five consecutive days, antagomir-27b-treated mice took a shorter time to find the platform from the third to fifth days compared with the MCAo group ($P < 0.05$, Fig. 3B). In the probe trial session, swimming time within the target quadrant was low in the MCAo group, which indicated that spatial memory of these mice was impaired after stroke. The antagomir-27b group showed a longer swimming time in the target quadrant than the MCAo group ($P < 0.05$, Fig. 3C, D). These data strongly indicated that antagomir-27b improved neurological function recovery of ischemic stroke mice.

During the study period, the mortality rate of the MCAo group was 17%, and treatment with antagomir-27b showed no obvious effect (Fig. 3E). Before sacrifice, the CBF in both the contralateral and the ipsilateral half brain was measured. The ipsilateral/contralateral flow ratio of the antagomir-27b group was significantly higher than that of the MCAo group (78.4% vs 62.7%, $P < 0.05$, Fig. S1). TTC staining revealed that the brain infarct volume was obviously decreased after antagomir-27b (Fig. 3E,F).

Antagomir-27b enhanced neurogenesis in MCAo mice via activating AMPK

To explore the mechanism beneath the therapeutic effects of antagomir-27b on ischemic stroke mice, we further tested whether the regulation of AMPK activity would affect neurogenesis *in vivo*. Immunostaining of hippocampal sections demonstrated that cell proliferation in the subgranular zone (revealed by BrdU⁺ cell populations) showed newborn neurons were enhanced in the MCAo group. The treatment of antagomir-27b significantly increased the number of BrdU⁺ cells by 44.5% compared with the MCAo group (Fig. 4A–D). Consistent with this, we observed an increase in cells expressing DCX, a marker of newly generated neurons, in DG (2.01-fold, Fig. 4E–H), CA3 (2.16-fold, Fig. 4I–L) and SVZ (1.93-fold, Fig. 4M–P) in the antagomir-27b-treated group. These data indicate that neurogenesis was improved and this process could at least partially explain the improvement of neurological function in antagomir-27b group. Western blotting demonstrated the expression of p-AMPK α 2 and p-PKC ζ/λ was significantly enhanced in DG and SVZ from the antagomir-27b group (Fig. 4S,T).

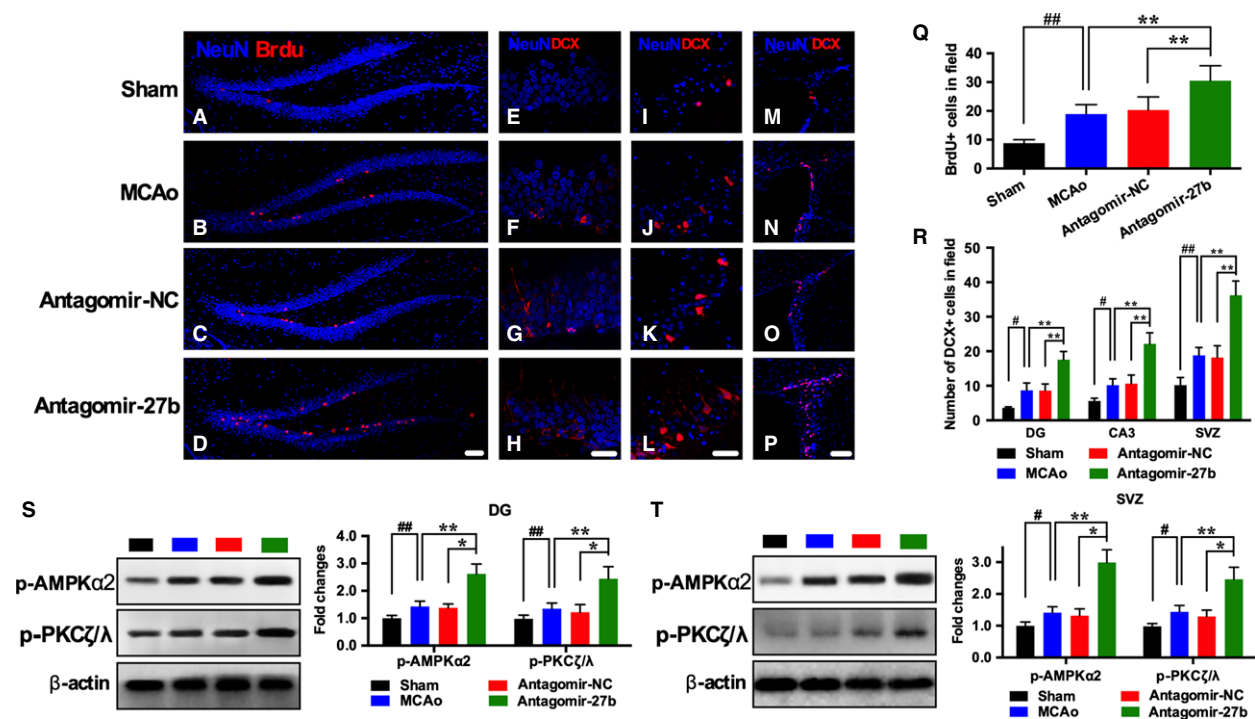


Fig. 4. Antagomir-27b improved neurogenesis in DG and SVZ after MCAo. (A–D, Q) Representative images and quantification of NeuN (blue) and BrdU (red) positive cells in DG. Scale bar = 100 μ m. Representative images and quantification of NeuN (blue) and DCX (red) positive cells in DG (E–H, R; scale bar = 50 μ m), CA3 (I–L, R; scale bar = 50 μ m) and SVZ (M–P, R; scale bar = 100 μ m). (S, T) Western blot analysis of p-AMPK α 2 and p-PKC ζ/λ expression and their quantitative data in DG (S) and SVZ (T). $n = 5$ /group. The data are expressed as mean \pm SEM. # $P < 0.05$, ## $P < 0.01$ vs Sham; * $P < 0.05$, ** $P < 0.01$ vs antagomir-27b (one-way ANOVA followed by *post hoc* Tukey's test).

Discussion

In the present study, we report that the inhibition of miR-27b improved neurogenesis in DG and SVZ via activating AMPK, and enhanced post-stroke recovery in a mouse MCAo model, which may become a potential therapeutic option for ischemic stroke.

Ischemic stroke, accounting for ~80% of stroke, leads to a high mortality rate and causes irreversible disability. Nowadays, the only FDA-approved cure, recombinant tissue plasminogen activator, has a narrow therapeutic window, which means that only ~4% patients receive the treatment in time [38]. Owing to their high metabolism rate, high oxygen consumption and low energy storage, neurons are vulnerable to damage under conditions of ischemia and hypoxia. AMPK is a known as a sensor and regulator of energy balance. When cellular energy supply is low, as signaled by increasing AMP/ATP, AMPK is activated and regulates metabolism by directly targeting metabolic enzymes and by regulating gene transcription.

Whether AMPK plays a beneficial or a detrimental role in ischemic brain has engendered considerable

controversy. It is newly recognized that AMPK activation can lead to different outcomes depending on the physiological status of the organism, and AMPK activation can protect the heart, endothelial cells, and smooth muscle cells under certain stress conditions [39,40]. Other groups reported that, short-term AMPK activation improved cell survival since it induced nuclear translocation of forkhead box O3 (FOXO3), while long-term of AMPK activation leads to cell death via stimulating a second activation step of FOXO3 and increasing Bim expression [41]. In our study, we confirmed miR-27b directly targets AMPK mRNA. When expression of miR-27b was inhibited, AMPK activity was stimulated in a mild and gradual manner, without affecting the neuronal survival in the hypoxic condition but improved NSC proliferation and differentiation into neurons *in vitro*.

Neurogenesis in DG and SVZ is involved in neuronal repair after ischemic stroke. Neuroblasts from the SVZ migrate to the damaged areas and serve as a replacement of the dead neurons and help the restoration of cognition and motor skills [42]. Metformin, a first-line drug prescribed for type 2 diabetes and a

well-established AMPK activator, has been proven to exert beneficial effects on stroke patients and to increase hippocampal neurogenesis in preclinical studies via the atypical protein kinase C (aPKC)-CREB-binding protein (CBP) pathway [43–45]. However, it has not been clarified whether the direct regulation of AMPK activity by miRNAs would affect neurogenesis. Increasing evidence has suggested that miRNAs participate in the cellular response to ischemic stroke injury [46–48]. In our study, inhibition of miR-27b enhanced both AMPK and p-AMPK expression levels, but did not change the p-AMPK/AMPK ratio, which differed from the mechanism of AICAR or metformin. To repair stroke-induced cell damage, a series of energy-consuming pathways are activated, and an acute and high level of AMPK activation may further contribute to cell death. However, a chronic and low level of AMPK activation might accommodate the brain to metabolic stress and regulate related signaling pathways. In the present study, depressed miR-27b expression improved stroke outcome and spatial memory, and enhanced neurogenesis in DG and SVZ. In both areas, the aPKC-CBP pathway was activated, which may explain the newborn neuron promotion, but the mechanism beneath this still needs to be explored.

In conclusion, we reported for the first time that a mild activation of AMPK by anti-miR-27b induced neurogenesis and promoted post-stroke recovery. This study provides a strong experimental basis for the use of AMPK activator after ischemic stroke, which may become a potential therapeutic option.

Acknowledgements

This work was supported by Natural Science Foundation of Shandong province (grant no. ZR2015HQ023; ZR2016GM001). We appreciate the support from the department of Neurosurgery, Affiliated Hospital of Weifang Medical University. We are grateful to Mr Haiting Zhang and Ms Chengmei Zhang for assistance in laboratory animal care.

Conflict of interest

The authors declare no conflict of interest.

Author contributions

ZW did the experiments design and wrote the final draft of manuscript; YY did *in vitro* experiments and wrote part of the manuscript draft; ZZ did the animal surgery and treatments; KD did functional tests, immunostaining and image analysis.

References

- 1 Feigin VL, Norrving B and Mensah GA (2017) Global burden of stroke. *Circ Res* **120**, 439–448.
- 2 Chapman SN, Mehndiratta P, Johansen MC, McMurry TL, Johnston KC and Southerland AM (2014) Current perspectives on the use of intravenous recombinant tissue plasminogen activator (tPA) for treatment of acute ischemic stroke. *Vasc Health Risk Manag* **10**, 75–87.
- 3 Lindvall O and Kokaia Z (2010) Stem cells in human neurodegenerative disorders—time for clinical translation? *J Clin Invest* **120**, 29–40.
- 4 Briones TL, Suh E, Hattar H and Wadowska M (2005) Dentate gyrus neurogenesis after cerebral ischemia and behavioral training. *Biol Res Nurs* **6**, 167–179.
- 5 Zhao Y, Guan YF, Zhou XM, Li GQ, Li ZY, Zhou CC, Wang P and Miao CY (2015) Regenerative neurogenesis after ischemic stroke promoted by nicotinamide phosphoribosyltransferase-nicotinamide adenine dinucleotide cascade. *Stroke* **46**, 1966–1974.
- 6 Tobin MK, Bonds JA, Minshall RD, Pelligrino DA, Testai FD and Lazarov O (2014) Neurogenesis and inflammation after ischemic stroke: what is known and where we go from here. *J Cereb Blood Flow Metab* **34**, 1573–1584.
- 7 Liu J, Solway K, Messing RO and Sharp FR (1998) Increased neurogenesis in the dentate gyrus after transient global ischemia in gerbils. *J Neurosci* **18**, 7768–7778.
- 8 Goritz C and Frisen J (2012) Neural stem cells and neurogenesis in the adult. *Cell Stem Cell* **10**, 657–659.
- 9 Kaplan MS and Hinds JW (1977) Neurogenesis in the adult rat: electron microscopic analysis of light radioautographs. *Science* **197**, 1092–1094.
- 10 Kuhn HG, Dickinson-Anson H and Gage FH (1996) Neurogenesis in the dentate gyrus of the adult rat: age-related decrease of neuronal progenitor proliferation. *J Neurosci* **16**, 2027–2033.
- 11 Barnea A and Nottebohm F (1994) Seasonal recruitment of hippocampal neurons in adult free-ranging black-capped chickadees. *Proc Natl Acad Sci USA* **91**, 11217–11221.
- 12 van Praag H, Kempermann G and Gage FH (1999) Running increases cell proliferation and neurogenesis in the adult mouse dentate gyrus. *Nat Neurosci* **2**, 266–270.
- 13 van Praag H, Christie BR, Sejnowski TJ and Gage FH (1999) Running enhances neurogenesis, learning, and long-term potentiation in mice. *Proc Natl Acad Sci USA* **96**, 13427–13431.
- 14 Li J, Zeng Z, Viollet B, Ronnett GV and McCullough LD (2007) Neuroprotective effects of adenosine monophosphate-activated protein kinase inhibition and gene deletion in stroke. *Stroke* **38**, 2992–2999.

- 15 McCullough LD, Zeng Z, Li H, Landree LE, McFadden J and Ronnett GV (2005) Pharmacological inhibition of AMP-activated protein kinase provides neuroprotection in stroke. *J Biol Chem* **280**, 20493–20502.
- 16 Li J, Benashski S and McCullough LD (2011) Post-stroke hypothermia provides neuroprotection through inhibition of AMP-activated protein kinase. *J Neurotrauma* **28**, 1281–1288.
- 17 Kuramoto N, Ito M, Saito Y, Niihara H, Tanaka N, Yamada K, Yamamura Y, Iwasaki K, Onishi Y and Ogita K (2013) Dephosphorylation of endogenous GABA(B) receptor R2 subunit and AMPK alpha subunits which were measured by in vitro method using transfer membrane. *Neurochem Int* **62**, 137–144.
- 18 Williams T, Courchet J, Viollet B, Brenman JE and Polleux F (2011) AMP-activated protein kinase (AMPK) activity is not required for neuronal development but regulates axogenesis during metabolic stress. *Proc Natl Acad Sci USA* **108**, 5849–5854.
- 19 Kobil T, Yuan C and van Praag H (2011) Endurance factors improve hippocampal neurogenesis and spatial memory in mice. *Learn Mem* **18**, 103–107.
- 20 Dagon Y, Avraham Y, Magen I, Gertler A, Ben-Hur T and Berry EM (2005) Nutritional status, cognition, and survival: a new role for leptin and AMP kinase. *J Biol Chem* **280**, 42142–42148.
- 21 Dp B (2004) MicroRNAs: genomics, biogenesis, mechanism, and function. *Cell* **116**, 281–297.
- 22 Liu SP, Fu RH, Yu HH, Li KW, Tsai CH, Shyu WC and Lin SZ (2009) MicroRNAs regulation modulated self-renewal and lineage differentiation of stem cells. *Cell Transplant* **18**, 1039–1045.
- 23 Xu W, Gao L, Zheng J, Li T, Shao A, Reis C, Chen S and Zhang J (2018) The roles of microRNAs in stroke: possible therapeutic targets. *Cell Transplant* **27**, 1778–1788.
- 24 Wang J, Chen T and Shan G (2017) miR-148b regulates proliferation and differentiation of neural stem cells via Wnt/beta-catenin signaling in rat ischemic stroke model. *Front Cell Neurosci* **11**, 329.
- 25 Wang N, Yang L, Zhang H, Lu X, Wang J, Cao Y, Chen L, Wang X, Cong L, Li J *et al.* (2018) MicroRNA-9a-5p alleviates ischemia injury after focal cerebral ischemia of the rat by targeting ATG5-mediated autophagy. *Cell Physiol Biochem* **45**, 78–87.
- 26 Zhang Q, Zhang K, Zhang C, Ge H, Yin Y, Feng H and Hu R (2017) MicroRNAs as big regulators of neural stem/progenitor cell proliferation, differentiation and migration: a potential treatment for stroke. *Curr Pharm Des* **23**, 2252–2257.
- 27 Yang X, Tang X, Sun P, Shi Y, Liu K, Hassan SH, Stetler RA, Chen J and Yin KJ (2017) MicroRNA-15a/16-1 antagomir ameliorates ischemic brain injury in experimental stroke. *Stroke* **48**, 1941–1947.
- 28 Liu B, Chen W, Cao G, Dong Z, Xu J, Luo T and Zhang S (2017) MicroRNA-27b inhibits cell proliferation in oral squamous cell carcinoma by targeting FZD7 and Wnt signaling pathway. *Arch Oral Biol* **83**, 92–96.
- 29 Kokovay E, Goderie S, Wang Y, Lotz S, Lin G, Sun Y, Roysam B, Shen Q and Temple S (2010) Adult SVZ lineage cells home to and leave the vascular niche via differential responses to SDF1/CXCR4 signaling. *Cell Stem Cell* **7**, 163–173.
- 30 Pachenari N, Kiani S and Javan M (2017) Inhibition of glycogen synthase kinase 3 increased subventricular zone stem cells proliferation. *Biomed Pharmacother* **93**, 1074–1082.
- 31 Yuan Y, Zhang Z, Wang Z and Liu J (2019) MiRNA-27b regulates angiogenesis by targeting AMPK in mouse ischemic stroke model. *Neuroscience* **398**, 12–22.
- 32 Zhang Y, Ueno Y, Liu XS, Buller B, Wang X, Chopp M and Zhang ZG (2013) The microRNA-17-92 cluster enhances axonal outgrowth in embryonic cortical neurons. *J Neurosci* **33**, 6885–6894.
- 33 Liu C, Liang B, Wang Q, Wu J and Zou MH (2010) Activation of AMP-activated protein kinase alpha alleviates endothelial cell apoptosis by increasing the expression of anti-apoptotic proteins Bcl-2 and survivin. *J Biol Chem* **285**, 15346–15355.
- 34 Gotti B, Benavides J, MacKenzie ET and Scatton B (1990) The pharmacotherapy of focal cortical ischaemia in the mouse. *Brain Res* **522**, 290–307.
- 35 Li Y, Chopp M, Chen J, Wang L, Gautam SC, Xu YX and Zhang Z (2000) Intrastratial transplantation of bone marrow nonhematopoietic cells improves functional recovery after stroke in adult mice. *J Cereb Blood Flow Metab* **20**, 1311–1319.
- 36 Chen J, Sanberg PR, Li Y, Wang L, Lu M, Willing AE, Sanchez-Ramos J and Chopp M (2001) Intravenous administration of human umbilical cord blood reduces behavioral deficits after stroke in rats. *Stroke* **32**, 2682–2688.
- 37 Ou Z, Kong X, Sun X, He X, Zhang L, Gong Z, Huang J, Xu B, Long D, Li J *et al.* (2017) Metformin treatment prevents amyloid plaque deposition and memory impairment in APP/PS1 mice. *Brain Behav Immun* **69**, 351–363.
- 38 Lackland DT, Roccella EJ, Deutsch AF, Fornage M, George MG, Howard G, Kissela BM, Kittner SJ, Lichtman JH, Lisabeth LD *et al.* (2014) Factors influencing the decline in stroke mortality: a statement from the American Heart Association/American Stroke Association. *Stroke* **45**, 315–353.
- 39 Xu Q and Si LY (2010) Protective effects of AMP-activated protein kinase in the cardiovascular system. *J Cell Mol Med* **14**, 2604–2613.

- 40 Manwani B and McCullough LD (2013) Function of the master energy regulator adenosine monophosphate-activated protein kinase in stroke. *J Neurosci Res* **91**, 1018–1029.
- 41 Davila D, Connolly NM, Bonner H, Weisova P, Dussmann H, Concannon CG, Huber HJ and Prehn JH (2012) Two-step activation of FOXO3 by AMPK generates a coherent feed-forward loop determining excitotoxic cell fate. *Cell Death Differ* **19**, 1677–1688.
- 42 Zhang R, Zhang Z and Chopp M (2016) Function of neural stem cells in ischemic brain repair processes. *J Cereb Blood Flow Metab* **36**, 2034–2043.
- 43 IDF Clinical Guidelines Task Force (2006) Global guideline for type 2 diabetes: recommendations for standard, comprehensive, and minimal care. *Diabet Med* **23**, 579–593.
- 44 Wang J, Gallagher D, DeVito LM, Cancino GI, Tsui D, He L, Keller GM, Frankland PW, Kaplan DR and Miller FD (2012) Metformin activates an atypical PKC-CBP pathway to promote neurogenesis and enhance spatial memory formation. *Cell Stem Cell* **11**, 23–35.
- 45 Fatt M, Hsu K, He L, Wondisford F, Miller FD, Kaplan DR and Wang J (2015) Metformin acts on two different molecular pathways to enhance adult neural precursor proliferation/self-renewal and differentiation. *Stem Cell Reports* **5**, 988–995.
- 46 Ziu M, Fletcher L, Savage JG, Jimenez DF, Digicaylioglu M and Bartanusz V (2014) Spatial and temporal expression levels of specific microRNAs in a spinal cord injury mouse model and their relationship to the duration of compression. *Spine J* **14**, 353–360.
- 47 Wang Y, Huang J, Ma Y, Tang G, Liu Y, Chen X, Zhang Z, Zeng L, Wang Y, Ouyang Y-B *et al.* (2015)

MicroRNA-29b is a therapeutic target in cerebral ischemia associated with aquaporin 4. *J Cereb Blood Flow Metab* **35**, 1977–1984.

- 48 Zhang N, Zhong J, Han S, Li Y, Yin Y and Li J (2016) MicroRNA-378 alleviates cerebral ischemic injury by negatively regulating apoptosis executioner caspase-3. *Int J Mol Sci* **17**, 1427.

Supporting information

Additional supporting information may be found online in the Supporting Information section at the end of the article.

Fig. S1. Antagomir-27b improved CBF after MCAo. Quantitative data of CBF on day 28 after MCAo. The data are expressed as mean \pm SEM. $n = 5/\text{group}$. $###P < 0.001$ vs Sham; $*P < 0.05$ vs antagomir-27b (one-way ANOVA followed by *post hoc* Tukey's test).

Fig. S2. Antagomir-27b activated the expression of p-AMPK *in vivo*. (A,B) Time course of p-AMPK $\alpha 2$ expression in SVZ after one-time injection of antagomir-27b. $n = 3/\text{time point}$, mean \pm SEM. $*P < 0.05$, $**P < 0.01$ compared with the non-treated time point (one-way ANOVA followed by *post hoc* Tukey's test). (C–F) Western blot analysis of p-AMPK $\alpha 2$ and AMPK $\alpha 2$ expression and their quantitative data in cortex (C,D) and striatum (E,F). $n = 5/\text{group}$. The data are expressed as mean \pm SEM. $^{\#}P < 0.05$, $###P < 0.01$ compared with Sham group; $*P < 0.05$, $**P < 0.01$ vs antagomir-27b (one-way ANOVA followed by *post hoc* Tukey's test).